Supporting Information

Chlorosome-Inspired Synthesis of Templated Metallochlorin-Lipid Nanoassemblies for Biomedical Applications

Kenneth K. Ng,[‡ a,b], Misa Takada, [‡b,c], Kara Harmatys[b], Juan Chen[b], Gang Zheng[*a,b,c]

[a]Institute of Biomaterials and Biomedical Engineering, University of Toronto, Toronto, ON M5G 1L7, Canadvivoa

[b]Princess Margaret Cancer Centre and Techna Institute, University Health Network, Toronto, ON M5G 1L7, Canada

[c]Department of Chemistry, Osaka University, Osaka 560-0043, Japan

[‡]These authors contributed equally to this work.

Supporting Figures

Figure S15 UPLC monitoring of zinc insertion into MeO-chlorin lipid (10)

Table S1. Size measurements of 20% chlorin derivatives embedded within liposomes using dynamic light scattering. (A) Z-average measurements and (B) Polydispersity index.

Name	Z-average (d.nm)	PDI
Zn-MeO-chlorin acid	113.9±9.6	0.3±0.2
Zn-vinyl-chlorin lipid	101±2.3	0.09±0.05
MeO-chlorin lipid	105±1.6	0.09±0.08
Zn-MeO-chlorin lipid	96.0±3.9	0.10±0.04

Table S2. Fluorescence properties of zinc chlorin derivatives embedded within lipid nanovesicles.

Name	FL λ_{max} (nm)	Stokes Shift (nm)	Full width at half max (nm)
Zn-MeO-chlorin acid	664	1	24
Zn-vinyl-chlorin lipid	682	9	21
MeO-chlorin lipid	676	10	40
Zn-MeO-chlorin lipid	725	0	15

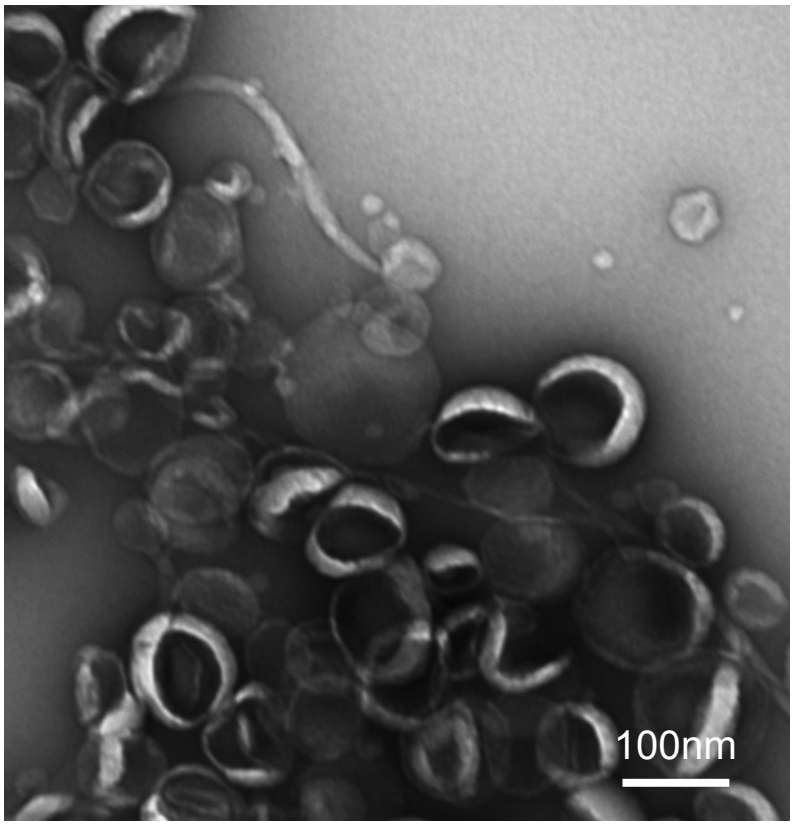

Figure S1. Transmission electron microscope image of lipid nanovesicles prepared with 20 mol % Zn-MeO-chlorin lipid.

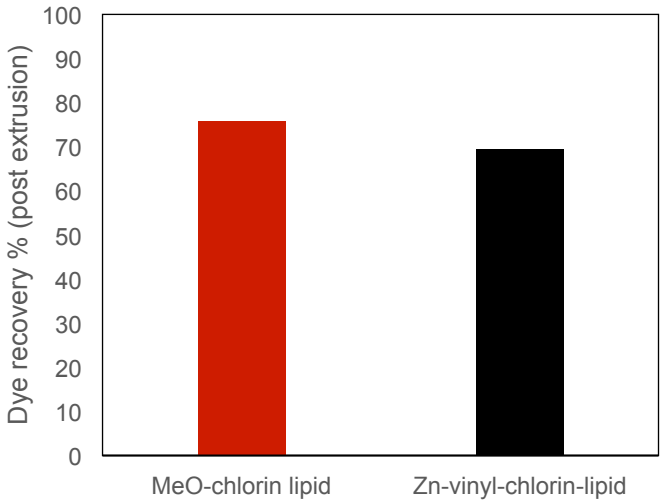

Figure S2. Effect of lipid conjugation on the incorporation of Zn-vinyl chlorin lipid (20%) and MeO-chlorin lipid (20%) compounds into lipid nanovesicles. Dye recovery

after extrusion in 20% chlorin lipid nanovesicle samples prepared using MeO-chlorin lipid (red) and Zn-vinyl-chlorin lipid (black).

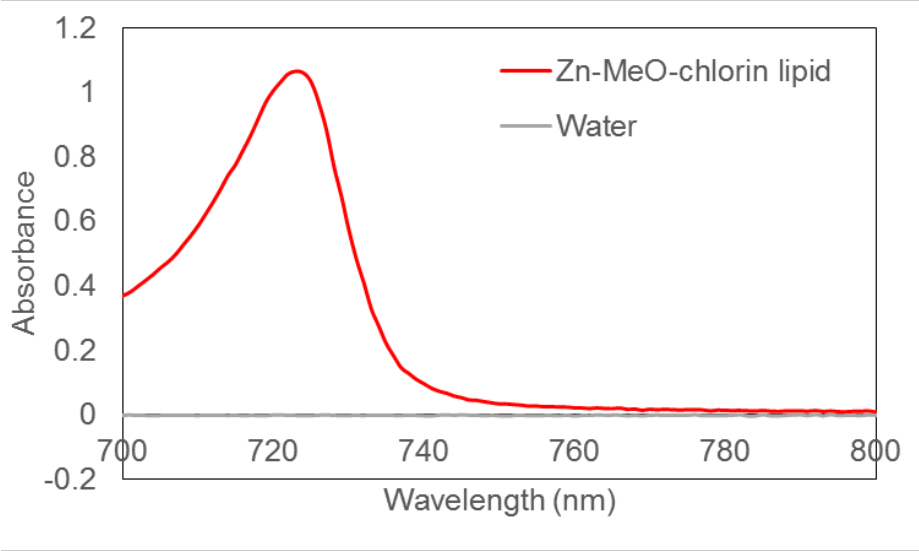

Figure S3. Absorption spectra of Zn MeO-chlorin lipid in water.

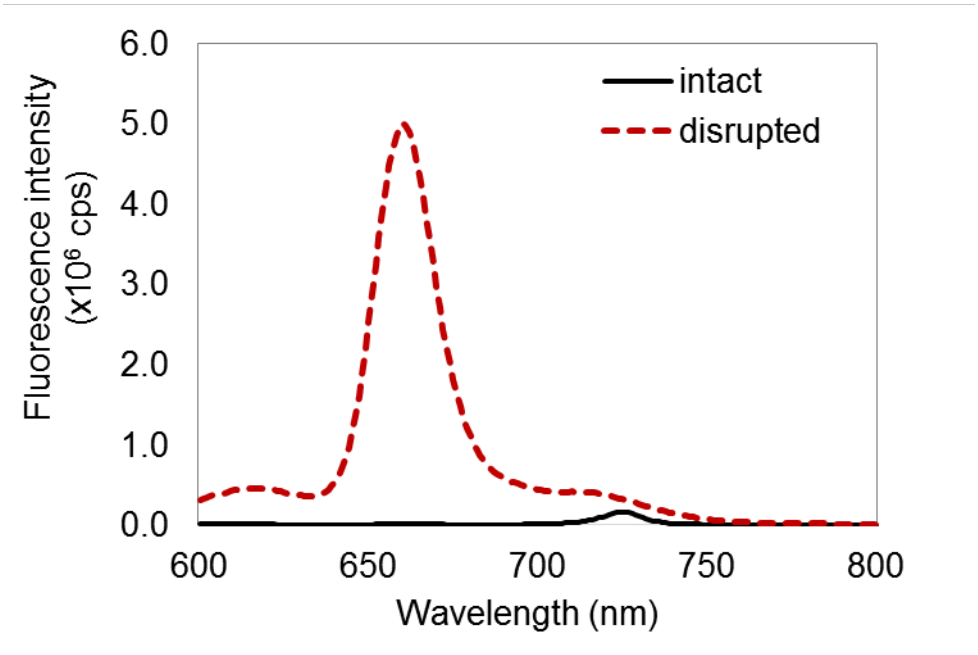

Figure S4. Fluorescence emission of 20 mol % Zn-MeO-chlorin lipid doped in lipid nanovesicles. Fluorescence emission from samples in the intact (black solid) and detergent-disrupted states (0.1% Triton X-100) (red dashed) demonstrating the structurally driven fluorescence quenching properties.

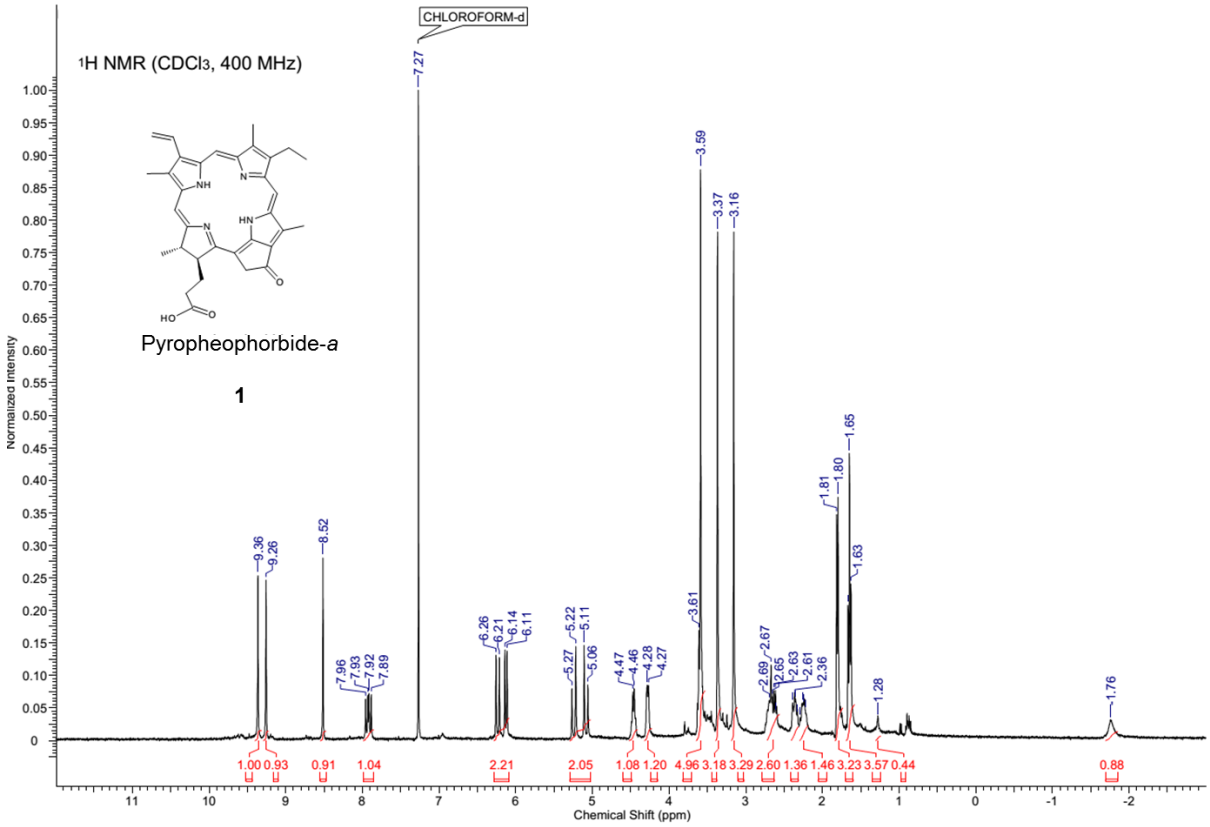

Figure S5 NMR spectrum for pyropheophorbide-*a* (1)

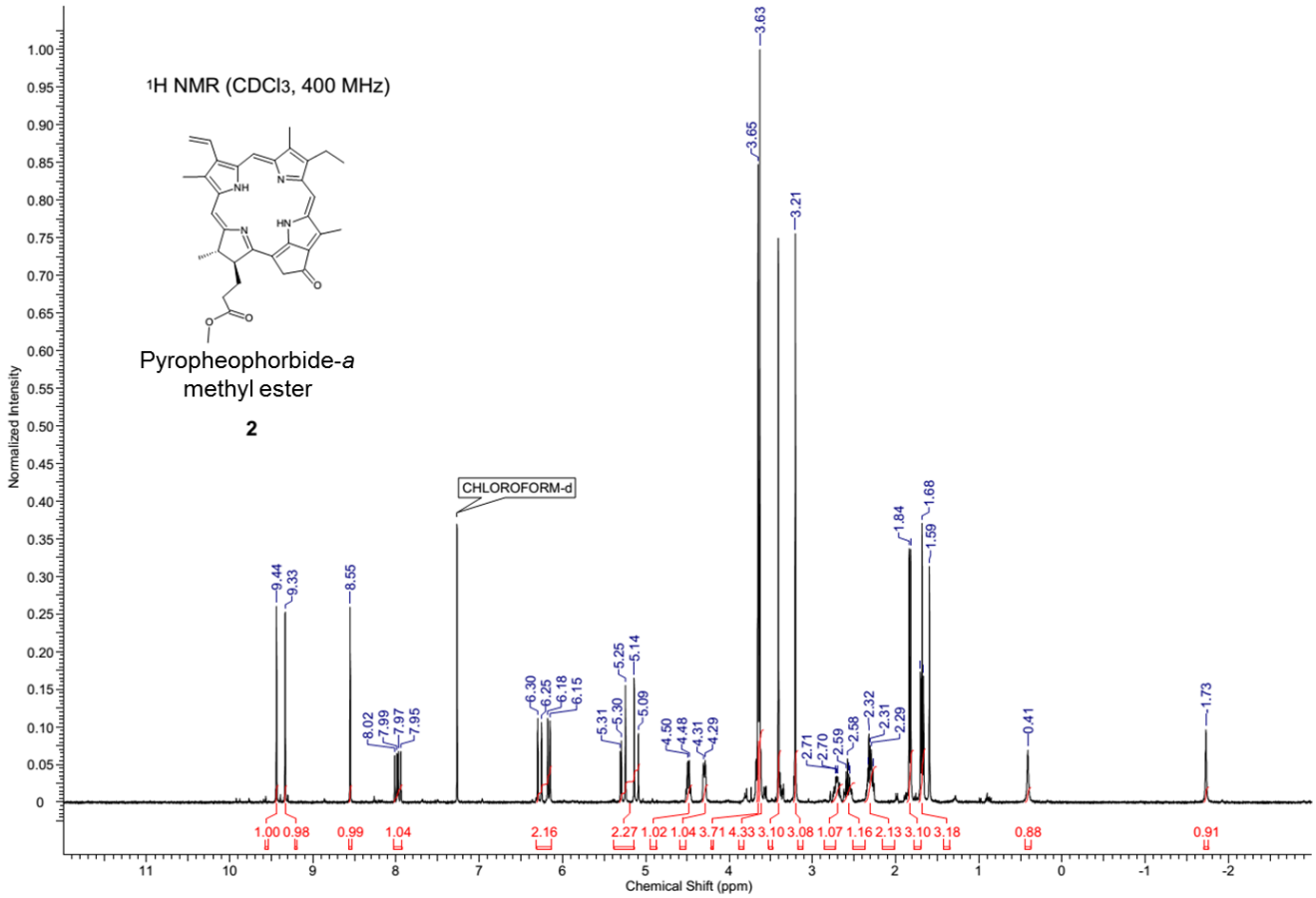

Figure S6 NMR spectrum for pyropheophorbide-*a* methyl ester (2)

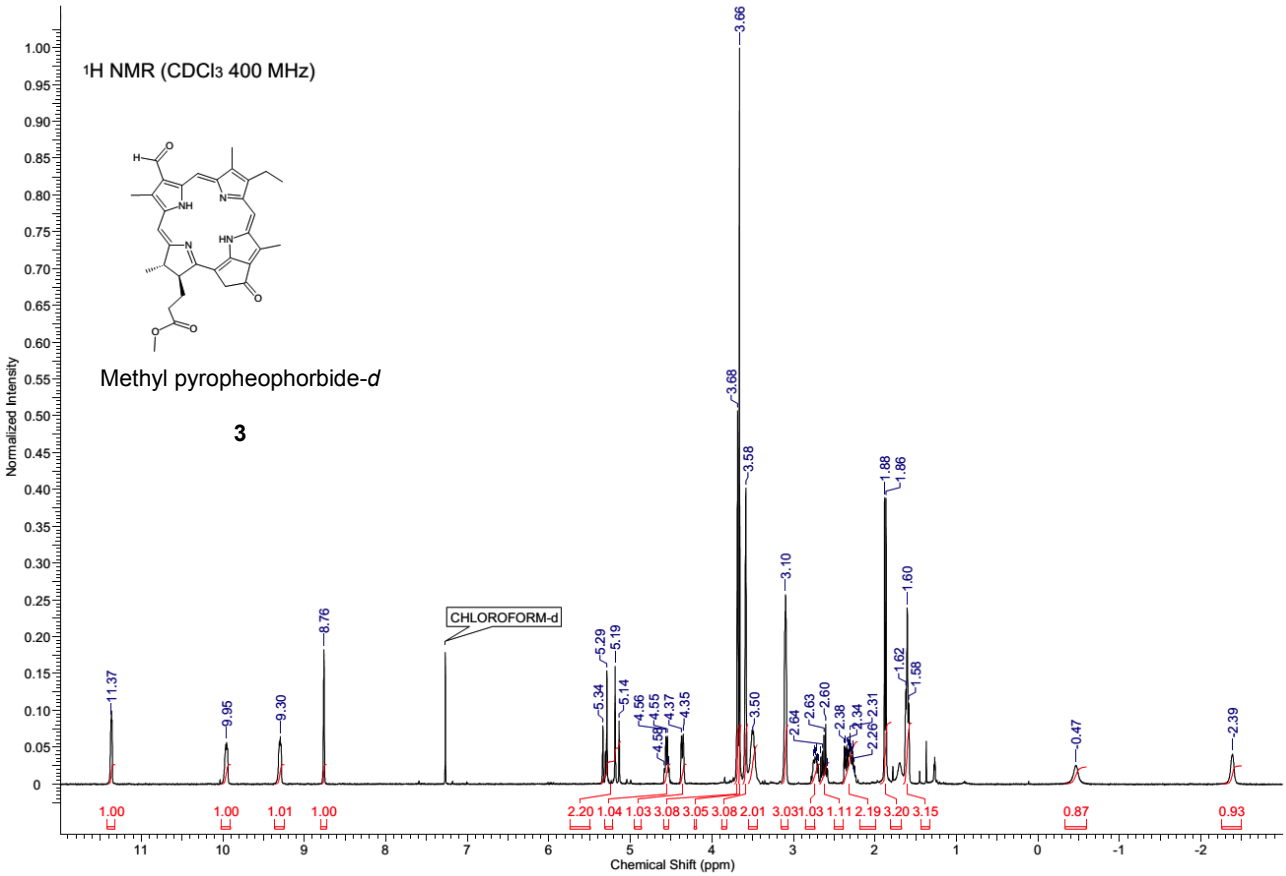

Figure S7 NMR spectrum for methyl pyropheophorbide-*d* (3)

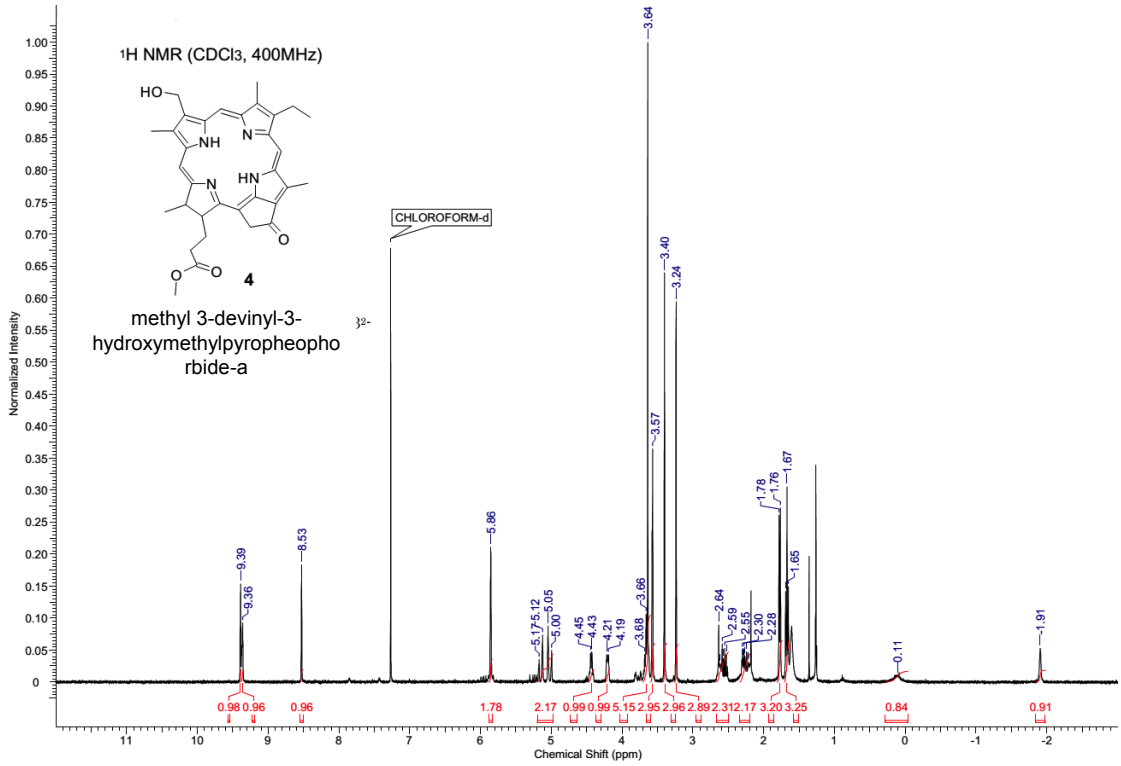

Figure S8 NMR spectrum for methyl 3-devinyl-3-hydroxymethylpyropheophorbide-*a* (4)

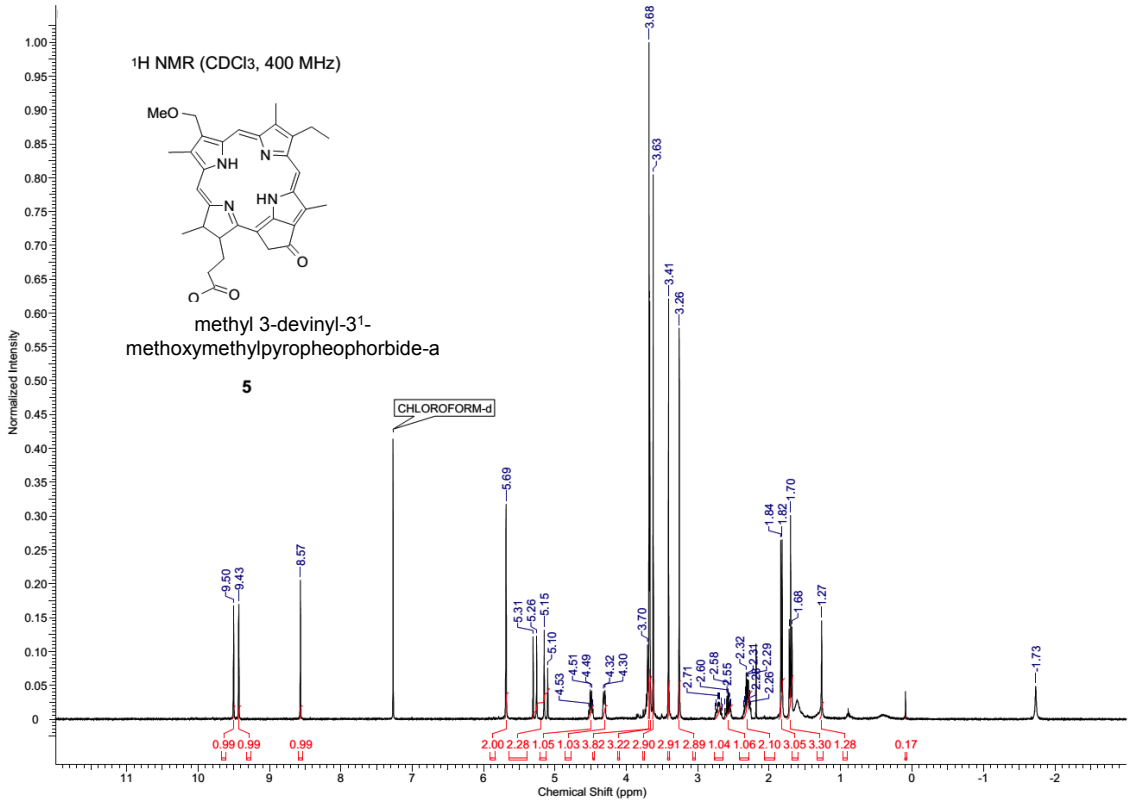

Figure S9 NMR spectrum for methyl 3-devinyl-3^1-methoxymethylpyropheophorbide-*a* (5)

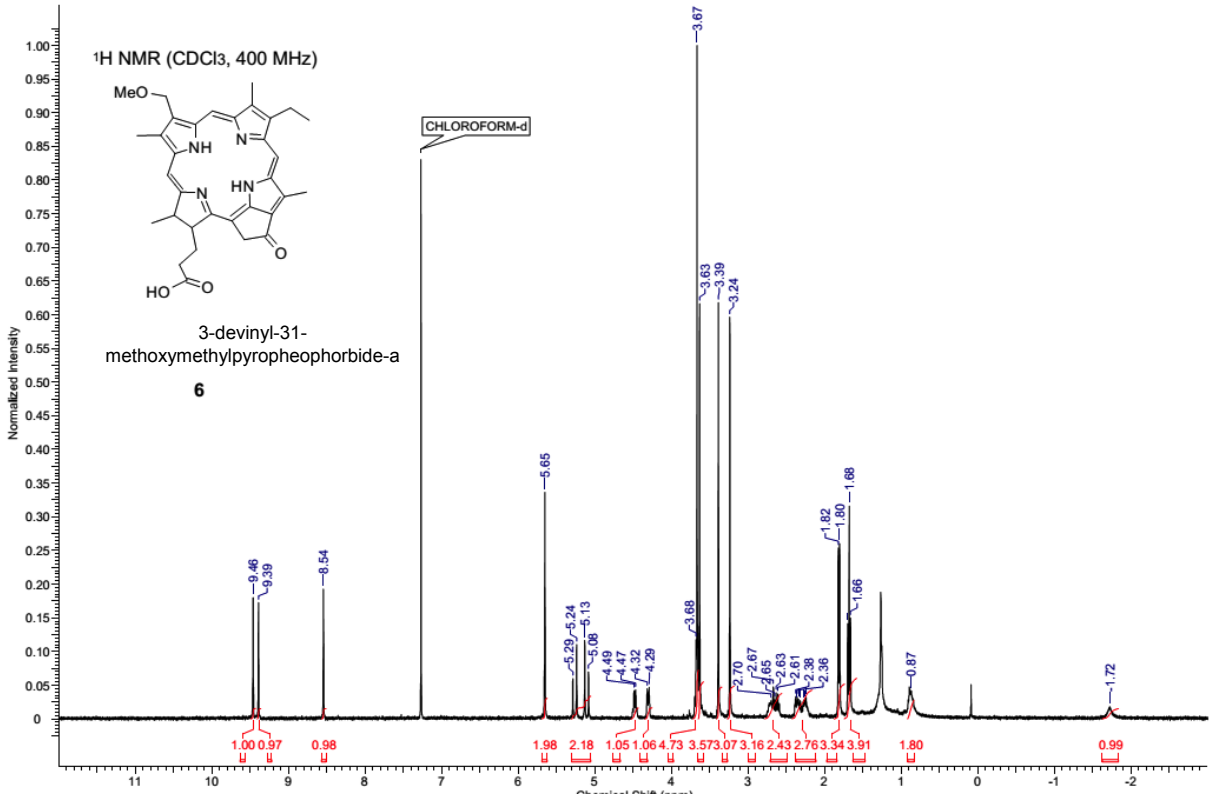

Figure S10 NMR spectrum for 3-devinyl-3[1]-methoxymethylpyropheophorbide-*a* (MeO-chlorin acid) (6)

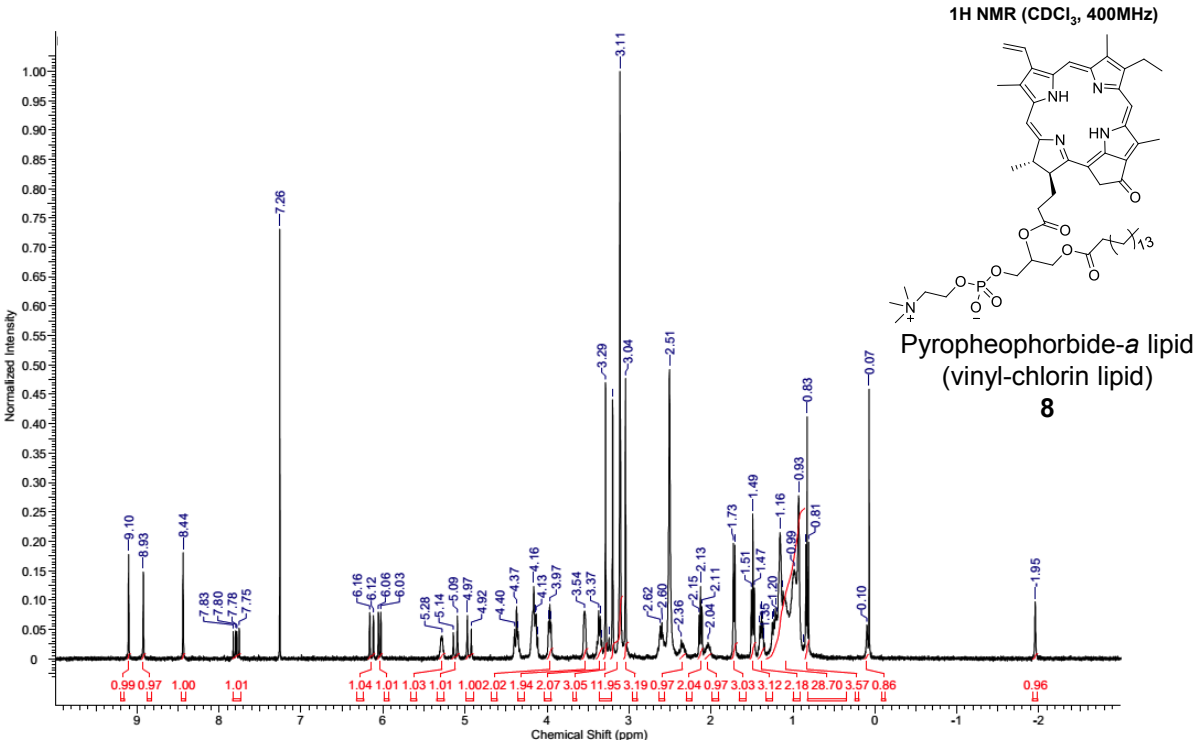

Figure S11 NMR spectrum for pyropheophorbide-*a* lipid (vinyl-chlorin lipid) (8)

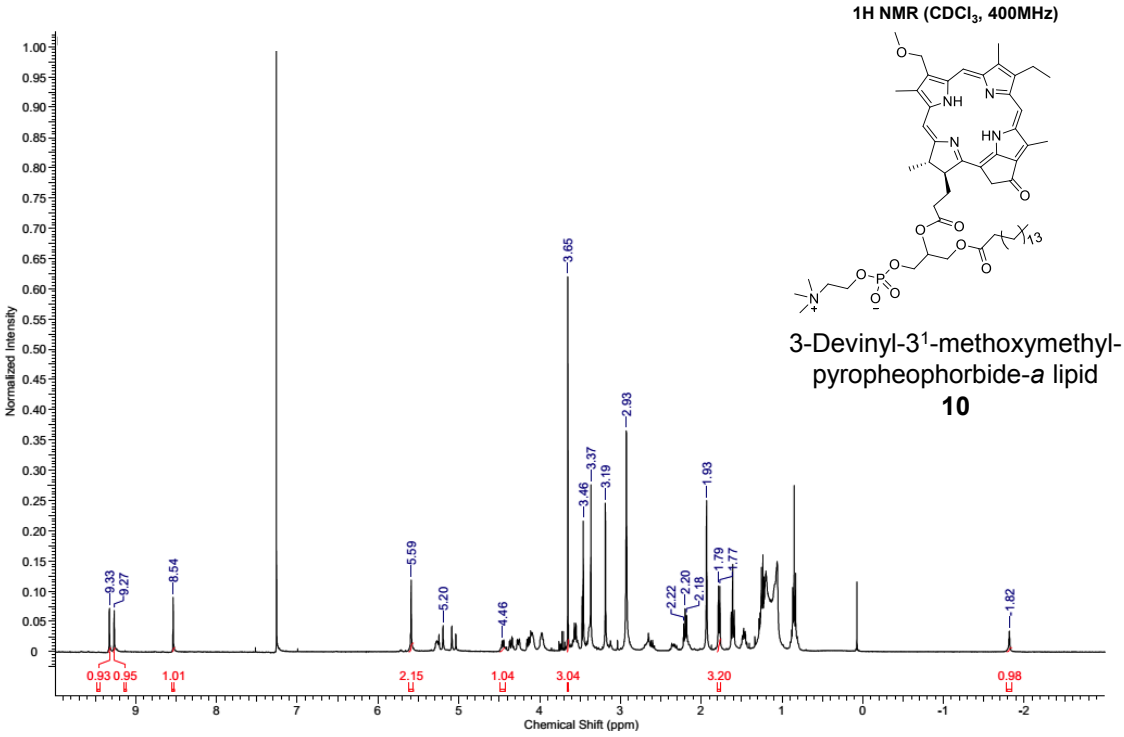

Figure S12 NMR spectrum for 3-Devinyl-3^{1}-methoxymethylpyropheophorbide-*a* lipid (MeO-chlorin lipid) (10)

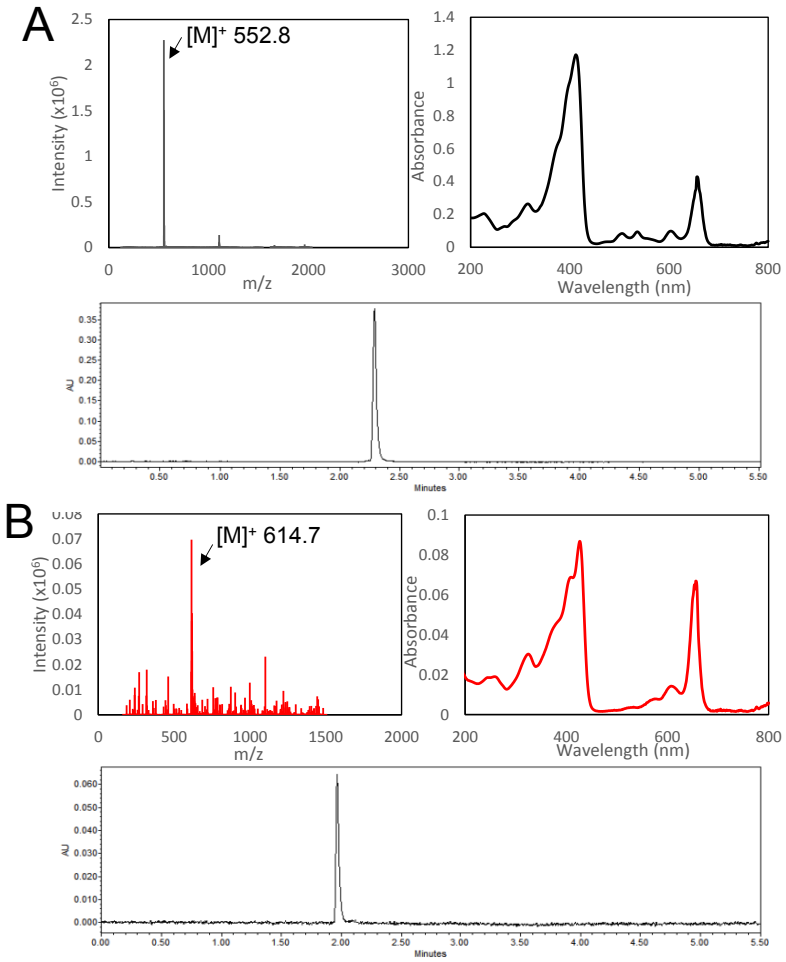

Figure S13 UPLC MS/UV data for MeO-chlorin acid (6) and Zn MeO-chlorin acid (7). (A) Mass spectrum, absorbance spectrum and UPLC chromatogram (655nm) of free base MeO-chlorin acid. (B) Mass spectrum, absorbance spectrum and UPLC chromatogram (655nm) of zinc-inserted MeO-chlorin acid.

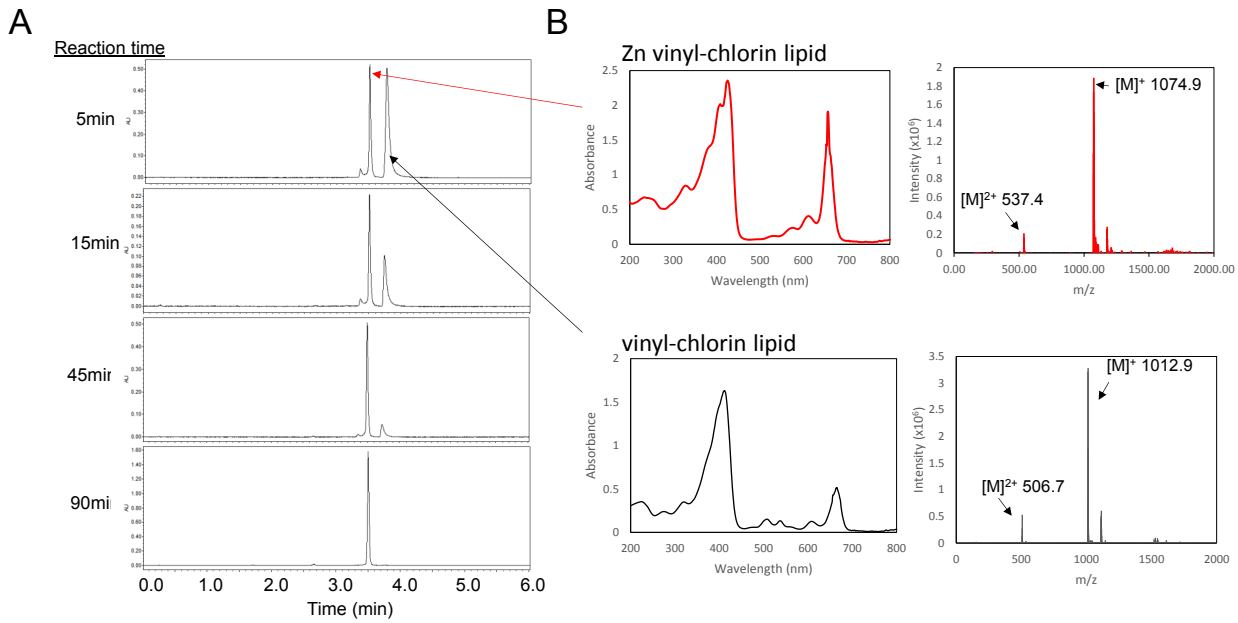

Figure S14 UPLC monitoring of zinc insertion into vinyl-chlorin lipid (8)

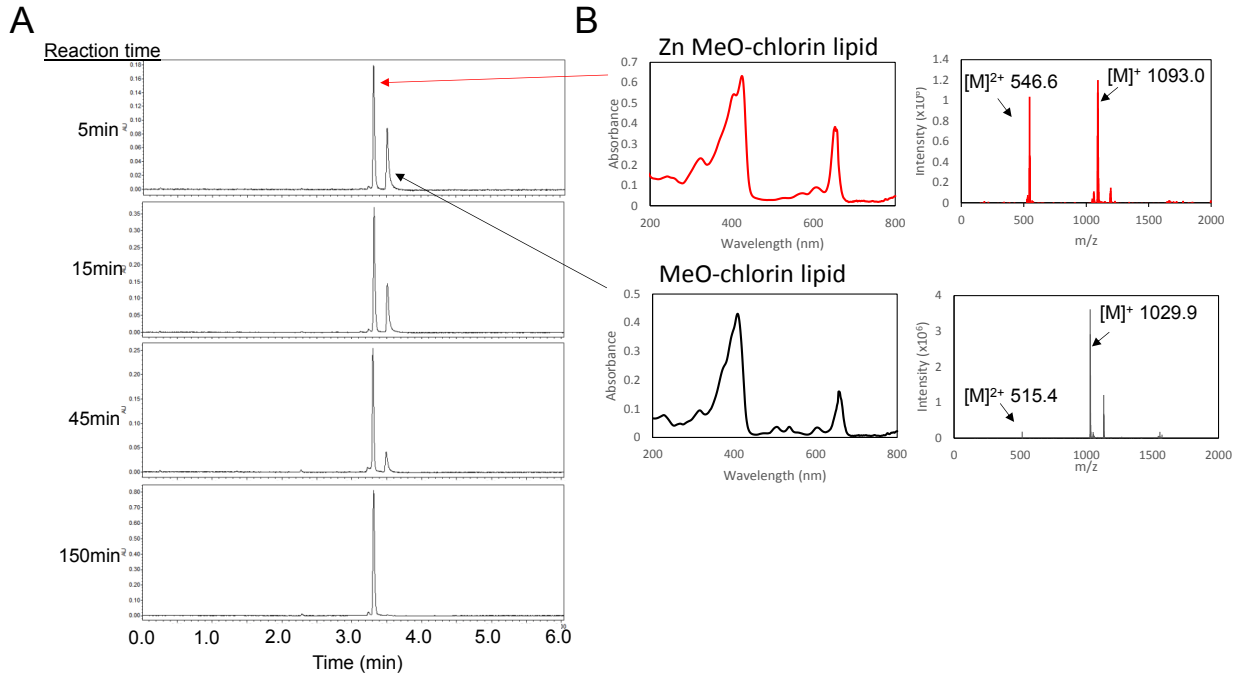

Figure S15 UPLC monitoring of zinc insertion into MeO-chlorin lipid (10)

Materials and methods

Materials

Dipalmitoylphosphatidylcholine (DPPC), 1,2-dipalmitoyl-sn-glycero-3-phosphoethanolamine-N-[methoxy(polyethylene glycol)-2000] (DPPE-mPEG2000), 1-hexadecanoyl-*sn*-glycero-3-phosphocholine (PHPC) were purchased from Avanti Polar Lipids, Inc. (Alabaster, AL) and other chemicals and solvents were purchased from Sigma Aldrich. Flash column chromatography was performed with silica gel 60 (230-400 um) (Merck) or with diol modified silica (Sorbtech). Proton nuclear magnetic resonance spectra were collected on a Bruker Ultra Shield 400 Plus (400 MHz). HPLC and mass spectrometry was conducted on Waters Micro Mass HPLC. Extruder drain discs and polycarbonate membranes were purchased from Whatman (Piscataway, NJ)

Methods

Particle characterization

Z-average size and polydispersity of the samples in PBS were measured using a Malvern ZS90 Nanosizer (Malvern Instruments, UK). Absorption spectra of each sample was determined by UV spectroscopy (CARY 50 UV/Vis S3 Spectrophotometer, Varian Inc.). Absorption spectra of intact samples was measured in PBS, and that of detergent disrupted samples was measured after adding Triton-X100 so that the final detergent concentration was 0.1% v/v. Transmission electron microscope images of negatively-stained (2% uranyl acetate) samples were conducted on a Hitachi H-7000 TEM using an acceleration voltage of 75 kV.

The ratio of the amount of zinc chlorin derivatives incorporated into the particles to that of initially loaded was also determined as dye recovery % by the following

equation:

$$\%\ \text{dye incorporated into nanovesicles} = \left(\frac{\text{ABS}_{658\ \text{nm}}(\text{after extrusion})}{\text{ABS}_{658\ \text{nm}}(\text{before extrusion})}\right)\times 100$$

where, ABS_{685nm}, is the absorbance at 658nm before extrusion and ABS_{685nm}, is the absorbance at 658nm after extrusion. These sample measurements were made by taking a small amount of sample before and after extrusion, each of which was dissolved by diluting 20 times in MeOH.

The color of Zn-MeO-chlorin acid (**7**) and Zn-MeO-chlorin lipid (**11**) nanoparticles was monitored after 10 freeze and thaw cycles. Concentration of chlorin dyes in each sample was adjusted to 60 μM. Samples were stored in the dark at room temperature for 10 days.

Fluorescence measurements were carried out on a Fluoromax-4 spectrofluorometer (Horiba Jobin Yvon, NJ) Fluorescence spectra of intact and detergent disrupted state was measured by exciting samples at 556 nm with a 5 nm slit width and collecting fluorescence from 600 nm to 800 nm with a 5 nm slit width. Quenching efficiency was calculated by the following equation:

$$\%\ \text{quenching efficiency} = \left(1 - \frac{F_0}{F_{\text{detergent}}}\right)\times 100$$

Where F_0 and $F_{detergent}$ are the integration of fluorescence intensity from 600 nm to 800 nm for intact and detergent-disrupted sample respectively. Circular dichroism spectra was measured in samples adjusted to the same concentration dispersed in PBS or in

PBS with 0.1% Triton-X100 using a J-815 Circular Dichroism Spectrometer (JASCO Inc.).

Photoacoustic signal detection

For photoacoustic signal measurements, PBS, Zn-MeO-chlorin lipid in PBS (for intact) or in 0.1% Triton-X100 (disrupted) were injected into polyethylene tubes (in. diam.: 0.381mm; out. diam.: 1.09; PE20; Intramedic, BD), which was then placed in a plastic holder filled with water. Signals were obtained using a Vevo 2100 LAZR photoacoustic imaging system (Fujifilm, Toronto, ON) equipped with a 21 MHz-centered transducer and a flashlamp-pumped Q-switched Nd:YAG laser. Photoacoustic spectra was measured from 680 to 970 nm with a 1 nm step size. In order to measure concentration dependency of photoacoustic signal of Zn-MeO-chlorin lipid (**11**), 5 different concentration was prepared. Optical density at the Q_y maxima of each sample in MeOH (653 nm) was adjusted to 0, 1.7, 3.3, 5.0, and 6.6. For this measurement, laser was set to 725 nm. Images were generated by scanning across the length of the tube and collecting the signal originating from the peak at 725 nm.